BIOLOGY OF REPRODUCTION **84,** 379–391 (2011)
Published online before print 6 October 2010.
DOI 10.1095/biolreprod.110.086231

Activin A Balances Sertoli and Germ Cell Proliferation in the Fetal Mouse Testis[1]

Sirisha H.S. Mendis,[3] Sarah J. Meachem,[4] Mai A. Sarraj,[4] and Kate L. Loveland[2,5,6,7]

Monash Institute of Medical Research,[3] Monash University, Clayton, Victoria, Australia
Prince Henry's Institute of Medical Research,[4] Clayton, Victoria, Australia
Departments of Biochemistry and Molecular Biology[5] and Anatomy and Developmental Biology,[6] Monash University, Clayton, Victoria
The Australian Research Council Centre of Excellence in Biotechnology and Development,[7] Australia

ABSTRACT

Activin affects many aspects of cellular development, including those essential for reproductive fitness. This study examined the contribution of activin A to murine fetal testicular development, revealing contrasting outcomes of activin actions on Sertoli cells and gonocytes. Shortly after sex determination, from Embryonic Day 12.5 (E12.5) through to birth (0 dpp), the activin A subunit transcript (*Inhba*) level rises in testis but not ovary, followed closely by the *Inha* transcript (encoding the inhibitory inhibin alpha subunit). Activin receptor transcript levels also change, with *Acvr1* (encoding ALK2) and *Acvr2b* (ActRIIB) significantly higher and lower, respectively, at 0 dpp compared with E13.5 and E15.5. Transcripts encoding the signaling mediators *Smad1*, *Smad3*, and *Smad4* were higher at 0 dpp compared with E13.5 and E15.5, whereas *Smad2*, *Smad5*, and *Smad7* were lower. Detection of phosphorylated (P-)SMAD2/3 in nearly all testis cell nuclei indicated widespread transforming growth factor beta (TGFB) and/or activin ligand signaling activity. In contrast to wild-type littermates, activin betaA subunit knockout (*Inhba*$^{-/-}$) mice have significantly smaller testes at birth, attributable to a 50% lower Sertoli cell number and decreased Sertoli cell proliferation from E13.5. *Inhba*$^{-/-}$ testes contained twice the normal gonocyte number at birth, with some appearing to bypass quiescence. Persistence of widespread P-SMAD2/3 in *Inhba*$^{-/-}$ cells indicates other TGFB superfamily ligands are active in fetal testes. Significant differences in *Smad* and cell cycle regulator transcript levels correlating to *Inhba* gene dosage correspond to differences in Sertoli and germ cell numbers. In *Inhba*$^{-/-}$ testes, *Cdkn1a* (encoding p21^{cip1}), identified previously in fetal gonocytes, was lower at E13.5, whereas *Cdkn1b* (encoding p^{27kip1} in somatic cells) was lower at birth, and cyclin D2 mRNA and protein were lower at E15.5 and 0 dpp. Thus, activin A dosage contributes to establishing the balance between Sertoli and germ cell number that is ultimately required for adult male fertility.

activin, activin signaling, cell cycle, developmental biology, gametogenesis, gene expression, gonocyte, Sertoli cells, spermatogenesis

INTRODUCTION

The transforming growth factor beta (TGFB) superfamily of ligands, including TGFBs, activins, bone morphogenetic proteins (BMPs), nodal, and growth and differentiation factors (GDFs), provides a complex set of signals that underpin germ cell development in both sexes [1–3]. The activins are formed by dimerization of two β subunits. Three activin proteins, activin A ($\beta_A\beta_A$ dimer), activin B ($\beta_B\beta_B$ dimer), and activin AB ($\beta_A\beta_B$ dimer), are best known for their endocrine functions. The inhibins, which antagonize activin actions, arise from the dimerization of a β subunit with a common inhibin α subunit to form inhibin A ($\alpha\beta_A$) or inhibin B ($\alpha\beta_B$). The activins and inhibins were discovered as gonadal peptides that either stimulated or inhibited, respectively, follicle-stimulating hormone release from the pituitary [4]. The major gonadal site of inhibin synthesis in males is the Sertoli cell, whereas in females this is restricted to granulosa cells. Several other proteins known to bind activin are also produced in gonads, including follistatin, follistatin-like 3, and Bambi, which, together with inhibin, regulate activin signaling outcomes (reviewed in Itman et al. [1]). Activin A has been implicated in many processes relating to testicular cell development, predominantly using in vitro approaches. The present study investigates how the lack of activin A in the *Inhba*$^{-/-}$ mouse affects development in the embryonic and newborn testis.

In mammals, male germ cells are specified to become gonocytes at the time of sex determination, following SRY expression by pre-Sertoli cells [5, 6]. Their exposure to prostaglandin D2, anti-Müllerian hormone (AMH), and testosterone from surrounding somatic cells around Embryonic Day 11.5 (E11.5) in the mouse ensures they will ultimately develop into spermatozoa [7, 8]. Murine gonocytes proliferate until around E14.5, arrest in G_0 of the cell cycle [9], and resume mitosis within the first 24 h after birth. At this time the gonocytes move from their central position in the seminiferous cord, where they are completely embedded in Sertoli cells, to contact the peripheral basement membrane, and they are now regarded as spermatogonia. Among these germ cells is the newly formed spermatogonial stem cell population which self-renews, expands through mitosis, and subsequently differentiates through meiosis to eventually yield mature spermatozoa [10]. This study focuses on the window of testis development from just after sex determination until birth.

Several studies have provided evidence that activin β_A and other TGFB superfamily ligands influence testis development during the fetal period of rapid growth following sex determination, affecting in particular gonocyte and Sertoli cell populations. An inhibitory affect of activin on total cell proliferation in fetal rat testis organ cultures has been reported previously [11], whereas TGFB1 and TGFB2 increased rat germ cell apoptosis in E13.5 testis organ cultures [12],

[1]Supported by National Health and Medical Research Council grants 545916 to K.L.L. and 545917 to K.L.L. and S.J.M.
[2]Correspondence: Kate L. Loveland, School of Biomedical Sciences, Level 1, STRIP Building 77, Monash University, Clayton, VIC 3800, Australia. FAX: 61 03 9902 9500; e-mail: kate.loveland@monash.edu

Received: 27 May 2010.
First decision: 29 June 2010.
Accepted: 22 September 2010.

eISSN: 1529-7268 http://www.biolreprod.org
ISSN: 0006-3363

implicating these pathways in the governance of germ cell development. In addition, activin A dosage affects growth of the fetal murine epididymis between E15.5 and E19.5 [13], and has the capacity to influence Sertoli cell proliferation and cord expansion in the mouse [14]. Our previous preliminary results [15] indicated that activin contributed to the suppression of germ cell numbers in the fetal testis, but the timing and mechanism by which this occurred were unknown.

Regulation of germ cell and Sertoli cell numbers in postnatal testes involves coordinated, progressive association of cyclins and specific cyclin-dependant kinase inhibitors that control cell cycle progression [16, 17]. The cell cycle inhibitors $p27^{kip1}$ and $p21^{cip1}$ inhibit postnatal Sertoli cell proliferation, and thus ultimately limit adult Sertoli cell numbers [18]. With regard to fetal gonocytes, there is evidence that production of proteins relating to the G_1–S cell cycle phase is under transcriptional control. Between E12.5 and E15.5, both *Ccne1* and *Ccne2* (encoding cyclins E1 and E2) are reduced in germ cells, whereas *Ccnd1*, *Ccnd2*, and *Ccnd3* (encoding cyclins D1–D3) are predominantly present in somatic cells. During this time frame, germ cells both exhibit increasing levels of *Cdkn1b*, *Cdkn2a*, and *Cdkn2b* (encoding $p27^{kip1}$, $p16^{INK4a}$, and $p15^{INK4b}$, respectively) and have a higher level of *Cdkn1a* (encoding $p21^{cip1}$) relative to somatic cells as they exit the cell cycle [9]. However, the *Cdkn1b* transcript measured from E12.5 to E15.5 predominantly reflects its presence in somatic cells. Because activin A causes G_1 arrest in plasmacytic cells through suppression of cyclin D2 and activation of $p21^{cip1}$ [19], we hypothesized that activin may control germ and Sertoli cell proliferation in the fetal testis in a similar manner.

The present study examines how graded levels of activin A affect germ and Sertoli cells in the developing male embryo, leading to the identification of developmental ages and processes affected by the absence of activin A. In addition, changes in activity of known activin target genes measured using quantitative PCR (qPCR) were shown to relate to *Inhba* gene dosage, cell type, and embryonic age. For the first time, these data document the phenotype of germ and Sertoli cell growth in the $Inhba^{-/-}$ embryonic testis from E13.5 to birth and reveal the potential molecular events that mediate activin actions which ultimately generate a balance between somatic and germ cells.

MATERIALS AND METHODS

Animals

Pregnant Swiss mice were obtained after timed matings from Monash Central Animal Services to collect fetal testes and ovaries for PCR and whole-mount in situ hybridization analysis. The BA 192B mouse line, lacking the *Inhba* coding sequence [20], was maintained through heterozygote breeding, because $Inhba^{-/-}$ animals are neonatal lethal. These mice were housed at the Monash University Central Animal House and at Monash Medical Centre Animal Facility in accordance with the Australian Code of Practice for the Care and Use of Animals for Scientific Purposes (1997), with a 12L:12D cycle at 22°C and with food and water available ad libitum. For timed matings, heterozygous males were caged with heterozygous females for the night, and the visualization of a copulatory plug the next morning was recorded as E0.5. Natural birth occurred on E19–E20, which was counted as Day 0 postpartum (termed 0 dpp, or newborn). The study was approved by the Monash Medical Centre Animal Ethics Committee.

Tissue Collection and Preparation

Pregnant mice were killed by cervical dislocation, and the embryos were quickly removed from the uterus for dissection under a binocular microscope. Embryonic age was determined from paw morphology, whereas embryo sex was ascertained from gonad morphology. Newborn mice were collected as soon as possible after birth, weighed, and decapitated before excision of the testes, whereas fetal testes were dissected free from the mesonephros. For proliferation studies, bromodeoxyuridine (BrdU; 100 mg/kg; Sigma-Aldrich, St. Louis, MO) was administered subcutaneously to newborn animals or intraperitoneally to pregnant mice 2 h prior to killing. The right testis of each animal was immediately snap frozen on dry ice and stored at −80°C for RNA preparation, whereas the left testis was immersion fixed with Bouin solution for 5 h prior to weighing. For stereological analyses, one testis from 0 dpp and embryonic mice (E13.5 and E15.5) was processed into hydroxyethyl methacrylate resin (Technovit 7100; Kulzer and Co. GmBH, Friedrichsdorf, Germany) according to the manufacturer's instructions. Thick (25 μm) resin sections were cut (Leica RM 2165 Rotary Microtome; Leica Instruments GmbH, Nussloch, Germany) and collected in series onto slides before staining with periodic acid and Schiff reagents and counterstaining with Mayer hematoxylin for subsequent determination of cell number. Bouin-fixed testes were embedded in paraffin, and sections were cut at 4 μm and placed on SuperFrost Plus slides (Menzel-Glaser GmbH, Braunschweig, Germany) for immunohistochemistry. For whole-mount in situ analysis, embryos were dissected from pregnant mice at E16.5 in ice-cold diethyl pyrocarbonate-PBS (DEPC-PBS) and fixed in 4% paraformaldehyde. For RT-PCR, gonads were dissected free from the mesonephros, frozen immediately on dry ice, and stored at −80°C until RNA extraction.

Genotyping

A tail biopsy of 2 mm from every animal was collected and digested in 50 μl of lysis buffer (10 mM Tris-HCl [pH 8.5], 50 mM KCl, 0.1 mg/ml gelatin, 0.45% Nonidet P-40, 0.45% Tween 20, and 10 mg/ml of proteinase K [21]) at 55°C overnight and then placed at 90°C for 10 min. One microliter of lysate was used as a template for genotyping via PCR. The presence of one product at 338 bp indicated the $Inhba^{+/+}$ genotype, a single product at 250 bp indicated an $Inhba^{-/-}$ animal, and the presence of two products identified an $Inhba^{+/-}$ animal. Genotyping primers and PCR conditions are provided in Table 1.

Embryonic Testis Volume Determination

Individual testes from embryonic mice could not be weighed accurately on our balance, so testis volumes were determined for E13.5 and E15.5 samples using the Cavalieri principle fractionator method [22]. Briefly, every fourth hydroxy methacrylate testis section was encircled using the CASTGRID V1.60 (Olympus) software program, and a series of points were superimposed onto the video screen. The number of points that overlaid the testis section was totaled. The product of the area of the point (5739.54 μm^2), thickness, and interval yielded the fetal testis volume for that sample.

Whole-Mount In Situ Hybridization

Whole-mount in situ hybridization was carried out as previously described [23], with minor modifications using digoxigenin-labeled cRNAs to localize *Inhba* mRNA in paraformaldehyde-fixed embryos. Riboprobes were generated corresponding to a 370-bp region with 100% identity between rat and mouse and used previously for Northern blots and in situ hybridization to detect *Inhba* [24].

Immunohistochemistry

Paraffin-embedded sections were used for all immunohistochemical analyses. Antibodies recognizing BrdU and proliferating cell nuclear antigen (PCNA; DAKO, Carpinteria, CA) were used to detect proliferating cells, whereas antibodies recognizing ActRIIA, ActRIIB, cyclin D2 (Santa Cruz Biotechnology, Santa Cruz, CA), and P-SMAD2/3 (Cell Signaling Technology) were also employed (see Table 2 for antibody and protocol details). Briefly, sections were rehydrated through histolene and a graded ethanol series before undergoing antigen retrieval in 50 mM glycine (pH 3.5) or citrate (pH 6.0) at 90°C in a microwave (800 W) for 3 min on high and 7 min on low settings before cooling for at least 45 min at room temperature. Slides were next treated with 3% hydrogen peroxide for 5 min and washed in Tris-buffered saline (TBS) before addition of the appropriate blocking agent for PCNA, ActRIIA, ActRIIA, cyclin D2, and P-SMAD2/3 detection for at least 20 min. For BrdU detection, antigen retrieval was performed by immersing sections in 0.01 M sodium citrate buffer and heating in an 800-W microwave for 4 min on high and 6 min on low before being left to cool. Slides were next treated with 3% hydrogen peroxide for 5 min and washed in TBS before addition of the appropriate blocking agent for PCNA, ActRIIA, ActRIIA, cyclin D2, and P-SMAD2/3 detection for at least 20 min. For BrdU detection, sections were then subjected to treatment with heat-activated 0.01% trypsin for 90 sec. For PCNA and BrdU localization, the primary antibody was diluted in DAKO Antibody Diluent (to 1.42 μg/ml and 4.4 μg/ml, respectively) and applied to sections for 2

TABLE 1. Primers used for genotyping and qPCR.[a]

mRNA	Accession no.	Forward primer (5′–3′)	Reverse primer (5′–3′)	Annealing temp. (°C)	Amplicon size (bp)
Inhba genotyping	NM_008380	agccacactcctccacaatc	tggagtgtgatggcaaggtc	60	338
Hprt genotyping	NM_013556	tgctgacctgctggattaca	ctgcattgttttgccagtgt	55	205
Acvr2a	NM_007396	gggacgcatttctgaggata	tcctggaggcatcctactca	62	517
Acvr2b	NM_007397	cgactttgtggctgtgaaga	tcgttccacgtgatgatgtt	62	463
Acvr1a	NM_007394	ggctgctttcaggtttatgag	tactgcaaacaccaccgaga	62	201
Acvr1b	NM_007395	gcggtcactgacaccataga	gagtcttcttgatgcgcaga	62	397
Smad1	NM_008539	gcttcgtgaagggttgggg	cggatgaaataggattgtgggg	62	147
Smad2	NM_010754	gcaaatacggtagatcagtggg	cagttttcgattgccttgagc	62	179
Smad3	NM_016769	agttggacgagctggagaag	ggcagtagataacgtgaggga	62	128
Smad4	NM_008540	acacccgccaagtaatcgc	ggtggtagtgctgttatgatggt	62	252
Smad5	NM_008541	gtgtataaatcggcatgagtagctatcc	ggctttgagagcacaataacagtaaaacc	62	553
Smad7	NM_008543	gaaaccgggggaacgaattat	gcggttgtaaacccacacg	62	305
Ccnd2	NM_009829	atgctgctcttgacggaact	cctcacgacttcattgagca	62	333
Cdkn1a	NM_007669	cctggtgatgtccgacctg	ccatgagcgcatcgcaatc	62	103
Cdkn1b	NM_009875	agtcagcgcaagtggaattt	agtagaactcgggcaagctg	62	224
Trp53	NM_011640	gcgtaaacgcttcgagatgtt	tttttatggcgggaagtagactg	62	144
Amh	NM_007445	cgagctcttgctgaagttcc	tgaaacagcgggaatcagag	62	308
Inhba	NM_008380	ggagaacgggtatgtggaga	tggtcctggttctgttagcc	62	221
Actb	NM_007393	aggctgtgctgtccctgtat	aaggaaggctggaaaagagc	62	388
Rn18s (18S)	NR_003278.1	gtaacccgttgaaccccatt	ccatccaatcggtagtagcg	55	151

[a] All products have been sequence verified.

h at room temperature, whereas one control section lacking primary antibody was used for detection of nonspecific binding of the secondary antibody. Controls were uniformly negative. Bound primary antibody was detected with Vectastain ABC according to the manufacturer's instructions (Vector Laboratories, Burlingame, CA) and visualized using 3′3-diaminobenzidine (Sigma-Aldrich) according to the manufacturer's instructions. Slides were counterstained with a 1:1 dilution of Harris hematoxylin (Sigma-Aldrich) and dehydrated through ethanol and histolene before mounting and application of a coverslip with DPX (Fluka- Sigma-Aldrich).

Cell Number Estimates Using the Optical Disector

The optical disector stereological method [25] was used to determine the total number of cell nuclei per testis in resin sections. All measurements were performed using a 100× objective on an Olympus BX-50 microscope (Olympus, Tokyo, Japan). A microcator (D 8225; Heideinhain, Traunreut, Germany) that monitored scanned depth was attached to the microscope stage. The images were captured by a JVC TK-C1381 video camera coupled to a Pentium PC computer using a Screen Machine II fast multimedia video adapter (FAST, Hamburg, Germany). The software package, CASTGRID V1.60 (Olympus), was used to generate an unbiased counting frame superimposed on a video image. Fields were selected by a systematic uniform random sampling scheme as described previously [25, 26], with the use of a motorized stage (Multicontrol 2000; ITK, Lahnau, Germany). The final screen magnification was 2708-fold. Sertoli cells were identified by the presence of irregularly shaped nuclei, which were typically positioned close to the cord basement membrane and contained multiple nucleoli. Gonocytes were identified as relatively large, circular to ovoid cells with large circular nuclei, centrally located within the cord and embedded within Sertoli cells. Every fourth resin section was examined, with at least 200 Sertoli and 300 gonocyte cell nuclei counted in total per sample using an unbiased counting frame (626 μm^2). For each age and genotype, five individual samples were analyzed, with 10–15 sections counted at each age and genotype.

The proportions of PCNA- and BrdU-labeled cells were quantified from high-power (1000×) electronic images captured with a Leica DC200 camera coupled to a Leica DMR microscope using Leica IM50 image software (version 1.2; 1992) in a sequential manner that ensured images did not overlap. Collection of approximately 15–25 images per testis section was sufficient to sample the entire testis, with five individual samples counted for each age and genotype.

Messenger RNA Analysis by PCR

For quantitative analysis, total RNA was isolated from E13.5, E15.5, and 0 dpp BA mouse testes, and E12.5, E14.5, and E16.5 wild-type gonads of both sexes using the RNeasy Mini Extraction Kit, and was treated using DNA-free DNase Treatment and Removal Reagents (Ambion Inc., Austin, TX). For this analysis, at each age and genotype 5–10 independent samples were measured. Five hundred nanograms of total testis RNA was reverse transcribed using oligo$(dT)_{20}$ primers (Sigma-Aldrich) and SuperScript III enzyme (Invitrogen Life Technologies). Real-time PCR was performed using the Applied Biosystems 7900HT Sequence Detection System (Applied Biosystems, Foster City, CA) with SYBR Green I fluorescence detection of amplified products. The PCR primer sequences (Table 1) were selected using Primer Bank (http://pga.mgh.harvard.edu/primerbank/index.html) and Primer3 [27] programs for commercial oligonucleotide synthesis (Sigma-Aldrich).

Each 10-μl PCR reaction included 2 μl of DEPC (Sigma-Aldrich) water, specific forward and reverse primers (10 μmol/L), 5 μl of SYBR Green Dye (Applied Biosystems), and 2 μl of reverse-transcribed cDNAs (diluted 1:100 in DEPC water). All genes were analyzed by the $_{\Delta\Delta}$CT Livak method [28] using *Actb* as the reference gene for all samples, which was shown to be uniform between samples of the same age, independent of genotype. The PCR cycling conditions were as follows: 94°C for 10 min, 40 cycles of 94°C for 30 sec, 62°C for 30 sec, and 72°C for 30 sec, followed by a melting curve analysis (95°C, 60°C, and 95°C for 15 sec each). A reference cDNA from wild-type adult mouse ovary or mouse testis, depending on the target gene, was used to

TABLE 2. Antibody and protocol details.

Antibody	Host species	Supplier	Catalog no.	Blocking reagent[a]	Antigen retrieval[b]	Diluent[c]
ActRIIA	Goat polyclonal	Santa Cruz	Sc-5667	NRS	Glycine	TB; 1:50, 1:100
ActRIIB	Goat polyclonal	Santa Cruz	Sc-5665	NRS	Glycine	TB; 1:50, 1:100
BrdU	Mouse monoclonal	Sigma-Aldrich	B-2531	NSS	Citrate	DAKO antibody diluent; 1:500
Cyclin D2	Rabbit polyclonal	Santa Cruz	Sc-593	NSS	Citrate	TB
PCNA	Mouse monoclonal	DAKO	M08798	NRS	Glycine	TB; 1:800
P-SMAD 2/3	Rabbit polyclonal	Cell signalling	#3101	NSS	Glycine	TB; 1:1000

[a] NRS, normal rabbit serum; NSS, normal sheep serum.
[b] Glycine (3mM glycine in 1 × TBS pH 3.5), citrate (1× sodium citrate buffer, pH 6).
[c] TB (0.1% BSA in 1 × TBS).

generate standard curves for each primer set in 5-fold dilutions (range, 0.032–20.0 pg of cDNA). All samples were assayed in triplicate on 5–10 independent samples, and all samples from each age were converted to cDNA and analyzed simultaneously. The PCR melting curves were inspected to ensure that single PCR amplicons were obtained in each experiment, and product identity was confirmed by nucleotide sequencing. All transcript measurement histograms are presented relative to the E13.5 wild-type value, which is set to 1.

For *Inhba* qPCR analysis, total RNA was extracted from isolated gonads dissected free from the mesonephroi of E12.5, E14.5, and E 16.5 mouse testes. The cDNA was produced using 500 ng of RNA essentially as described above. Amplification was performed using Superscript II Taq polymerase (Invitrogen Life Technologies) on an Applied Biosystems 7900HT Sequence Detection System (Applied Biosystems, Foster City, CA). The PCR cycling conditions were 95°C for 10 min, 40 cycles each of 95°C for 30 sec of denaturation, 55°C for 5 sec of annealing, and 72°C for 13 sec of extension. Amplification products were analyzed on a 1.5% agarose gel, with a single amplification product of 338 bp (*Inhba*) obtained for each sample and a single amplification product of 151 bp for each *Rn18s* (loading control; Table 1). The PCR products were verified by cloning and sequencing. Three different sets of cDNA pools were used to perform replicates, each comprising 7–10 pairs of gonads from each sex. The PCR reactions were performed in triplicate with negative controls, where water was used in place of the reverse-transcribed template, included for each primer pair to exclude PCR amplification of contaminating DNA. *Inhba* mRNA levels were normalized to that of 18S as previously described [29] in detail.

Statistics

Statistical analysis was performed using a one-way ANOVA followed by a Newman-Keuls or Tukey post hoc test (Graph Pad PRISM Version 2.01). Once values had passed a normality test, differences were deemed significant at $P < 0.05$. Further analysis was then performed on individual data sets to check for potential litter effects within genotype group. This analysis revealed that there were no significant litter effects that might bias the results. The data are expressed as mean ± SEM.

RESULTS

Inhba *Expression in Whole Testes*

The sex-specific expression profile of *Inhba* was confirmed via RT-qPCR analysis of male and female gonads. Expression levels of *Inhba* in fetal testes were higher than those of the ovary, with transcript levels at E14.5 and E16.5 significantly elevated (Fig. 1A). Publicly accessible data (www.ncbi.gov/geo/) from Affymetrix analyses also indicate that after E12.5 the fetal testis expresses *Inhba* mRNA at increasingly higher levels compared with the sustained, low signal in fetal ovaries [30]. No *Inhba* transcript was visible by in situ hybridization in ovaries of E16.5 embryos (Fig. 1B), whereas a dark purple staining indicates this mRNA is present in testes. Signal in the kidneys of both samples served as a positive control. The presence of P-SMAD2/3 in almost all nuclei of the fetal testis at E13.5, E15.5, and 0 dpp (Fig. 1C) indicates that signaling through the TGFB/activin pathways is ubiquitous in cells of the fetal mouse testis.

Testis Weights and Volumes

Fetal testes at E13.5 and E15.5 could not be weighed accurately, so the fractionator method was employed to determine fetal testis volumes. Testes from 0 dpp animals

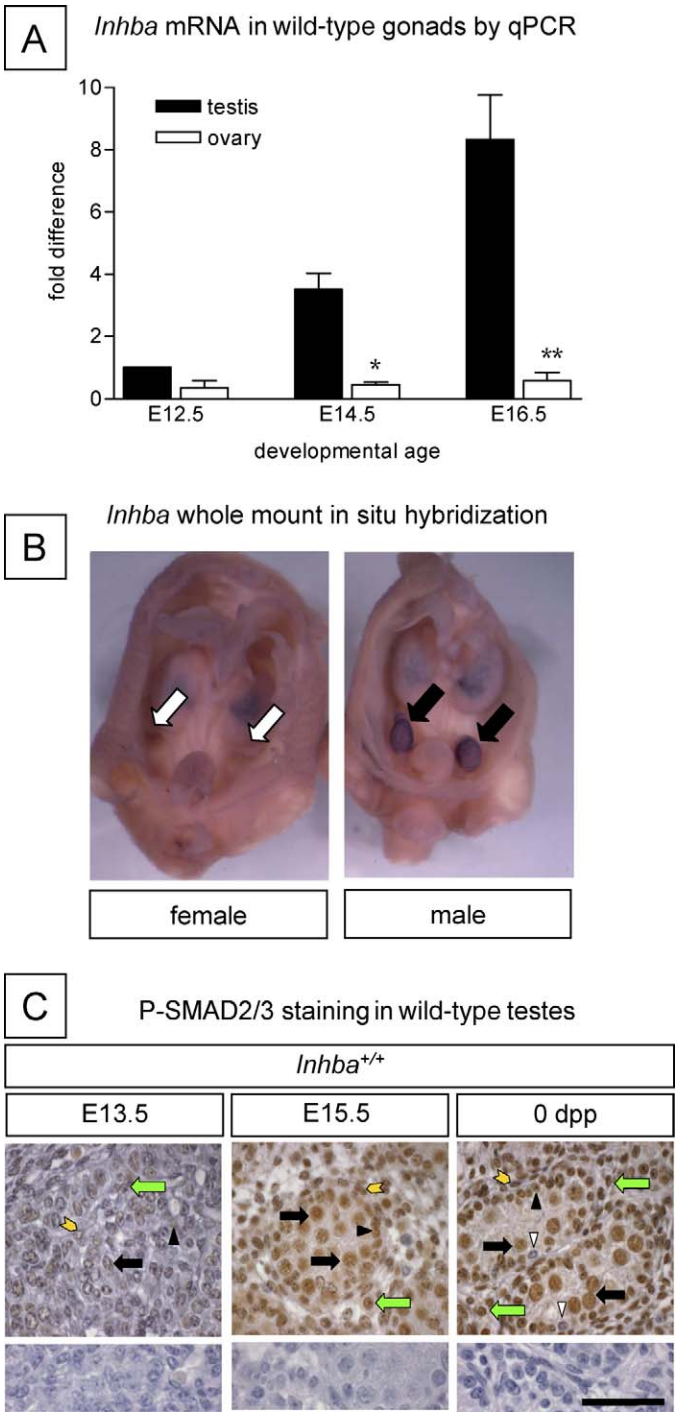

FIG. 1. Selective upregulation of *Inhba* subunit in the fetal testis. **A**) Quantitative PCR analysis of total fetal gonad mRNA confirms *Inhba* mRNA is sex specifically upregulated during testis development. Expression of *Inhba* in male gonads is higher at all ages analyzed, with significantly elevated levels at E14.5 (*$P < 0.05$) and E16.5 (**$P < 0.001$) compared with the ovary at corresponding ages by one-way ANOVA and Tukey multiple comparison post test. All samples have been normalized to housekeeping gene ribosomal 18S RNA (*Rn18s*) levels and are reported as a relative fold change from the E12.5 male value, which is assigned a value of 1. Data are represented as mean ± SEM from three pools, each consisting of 7–10 pairs of gonads from each sex, analyzed in triplicate. **B**) Whole-mount in situ hybridization of *Inhba* in fetal gonads. Female and male gonads at E16.5 are shown attached to hindquarters of an embryo. Embryonic ovaries were devoid of *Inhba* signal (white arrows), whereas intense *Inhba* signal was detected in the embryonic testis, represented as a dark purple stain (black arrows). **C**) P-SMAD2/3 in all cells of the wild-type fetal mouse testis. Representative images illustrating P-SMAD2/3 immunostaining in the wild-type testis at E13.5, E15.5, and 0 dpp. P-SMAD2/3 was detected in the nuclei of gonocytes (black arrows), Sertoli cell nuclei (black arrowheads), peritubular myoid cells (yellow chevrons), and interstitial cells (green arrows), whereas only a small number of Sertoli cell nuclei remained unstained (white arrowheads). Lower panels represent control sections incubated without primary antibody. All sections are counterstained blue with Harris hematoxylin, with a brown nuclear signal indicating positive reaction. Bar = 50 μm.

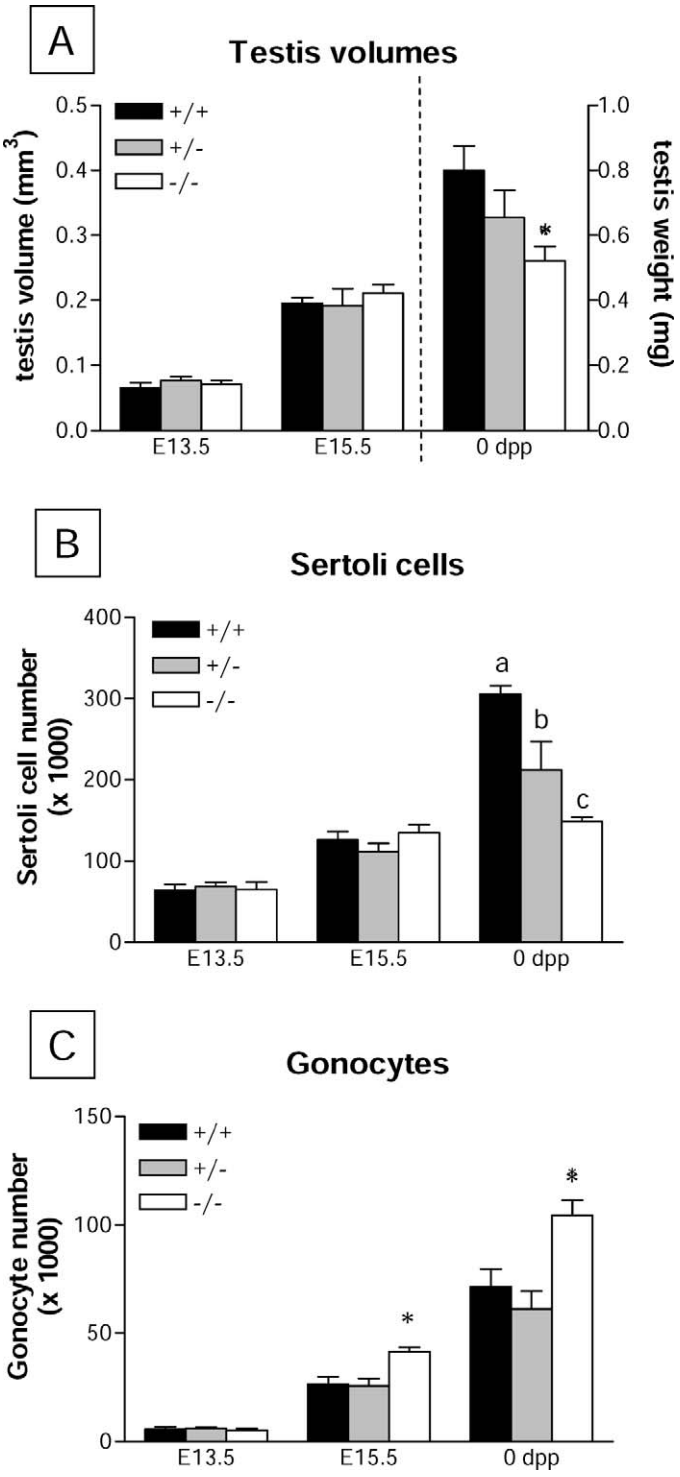

FIG. 2. *Inhba* dosage influences testis volume and cell numbers in the fetal testis. **A**) Testis volumes from animals of all three genotypes at E13.5, E15.5, and 0 dpp were determined. For E13.5 and E15.5, testis volume was determined using the fractionator method, whereas for newborn (0 dpp) animals, absolute testis weights were used. At 0 dpp, the $Inhba^{-/-}$ animal (white bars) exhibited significantly smaller testes compared with $Inhba^{+/+}$ littermates (black bars), whereas no differences were detected at fetal ages. *Significant differences ($P < 0.05$) by one-way ANOVA and Newman-Keuls post test. For all ages studied, n = 5 or 6 animals per genotype. **B**) Sertoli cell numbers did not differ relative to genotype at E13.5 and E15.5. At 0 dpp, however, Sertoli cell numbers in the $Inhba^{-/-}$ animal were significantly lower than in $Inhba^{+/+}$ (2-fold decrease) and $Inhba^{+/-}$ (1.4-fold decrease) littermates. $Inhba^{+/-}$ animals also had a lower number of Sertoli cells compared with $Inhba^{+/+}$ animals. Letters indicate statistically significant differences between genotype groups ($P <$ 0.05) by one-way ANOVA and Newman-Keuls post test. For all ages studied, n = 5 animals per genotype. **C**) Testicular gonocyte numbers were unchanged at E13.5 between animals of different genotypes. At E15.5 the $Inhba^{-/-}$ animal exhibited significantly higher numbers of gonocytes compared with $Inhba^{+/+}$ littermates ($P < 0.05$), and this was also measured at 0 dpp. *Significant differences ($P < 0.05$) by one-way ANOVA and Newman-Keuls post test. For all ages studied, n = 5 animals per genotype.

were weighed. Fetal testis volumes were not different between animals of different genotype at E13.5 and E15.5 (Fig. 2A); however, the testis weights of $Inhba^{-/-}$ animals were significantly lower than $Inhba^{+/+}$ at 0 dpp ($P < 0.05$).

Cell Number

Sertoli cell numbers at E13.5 and E15.5 were not different between genotypes; however, at 0 dpp $Inhba^{-/-}$ animals had significantly fewer Sertoli cells compared with $Inhba^{+/-}$ animals (30.7% lower). An even greater difference (51.5% lower) was detected when compared with $Inhba^{+/+}$ littermates (Fig. 2B).

Gonocyte numbers in the testis of E13.5 testes were the same in animals of different genotypes; however, the $Inhba^{-/-}$ animals at E15.5 had more gonocytes compared with $Inhba^{+/+}$ littermates ($P < 0.05$; Fig. 2C). Gonocyte numbers in 0 dpp $Inhba^{-/-}$ testes were increased by 146% relative to the $Inhba^{+/+}$ animals ($P < 0.01$) and by 170% compared with $Inhba^{+/-}$ animals ($P < 0.05$; Fig. 2C).

Cell Proliferation

Sertoli and germ cell proliferation were analyzed using two independent labeling methods, anti-BrdU and anti-PCNA, to identify the proportion of cells labeled with each method (Fig. 3 and Supplemental Fig. S1, available online at www.biolreprod.org). This study was initially undertaken to examine BrdU proliferation at the three ages. In retrospect, we realized there might be informative data available from looking at an intermediate age. Because we had E17.5 samples available from animals that had not been previously treated with BrdU, we chose to examine proliferation using PCNA on the full range of ages. *Inhba* gene dosage did not alter the percentage of BrdU-labeled Sertoli cells at E13.5 and E15.5 (Fig. 3A). At 0 dpp, however, $Inhba^{-/-}$ animals demonstrated a decrease in the percentage of BrdU-labeled Sertoli cells compared with both $Inhba^{+/+}$ and $Inhba^{+/-}$ animals ($P < 0.05$). PCNA labeling of Sertoli cells demonstrated significant differences at all three ages. At E13.5, significantly fewer PCNA-labeled Sertoli cells were recorded in $Inhba^{-/-}$ animals than in $Inhba^{+/-}$ samples, whereas no difference was observed compared with $Inhba^{+/+}$ samples (Fig. 3B). At E15.5 and 0 dpp, the percentage of PCNA-labeled Sertoli cells in $Inhba^{-/-}$ testes was significantly lower compared with both $Inhba^{+/+}$ and $Inhba^{+/-}$ animals ($P < 0.05$), whereas at E17.5 $Inhba^{+/-}$ samples showed differences compared with both $Inhba^{+/+}$ and $Inhba^{-/-}$ animals.

Inhba gene dosage did not significantly affect the percentage of BrdU-labeled gonocytes at any age analyzed (Fig. 3C). However, at E15.5, more dividing cells were obvious in testes of $Inhba^{-/-}$ animals compared with $Inhba^{+/+}$ and $Inhba^{+/-}$ samples, whereas at 0 dpp no BrdU incorporation was detectable. The percentage of PCNA-labeled gonocytes was not significantly affected by *Inhba* gene dosage at any age (Fig. 3D); however, gonocytes with PCNA were detected at E17.5 in $Inhba^{-/-}$ testes, suggesting that some cells continued to cycle.

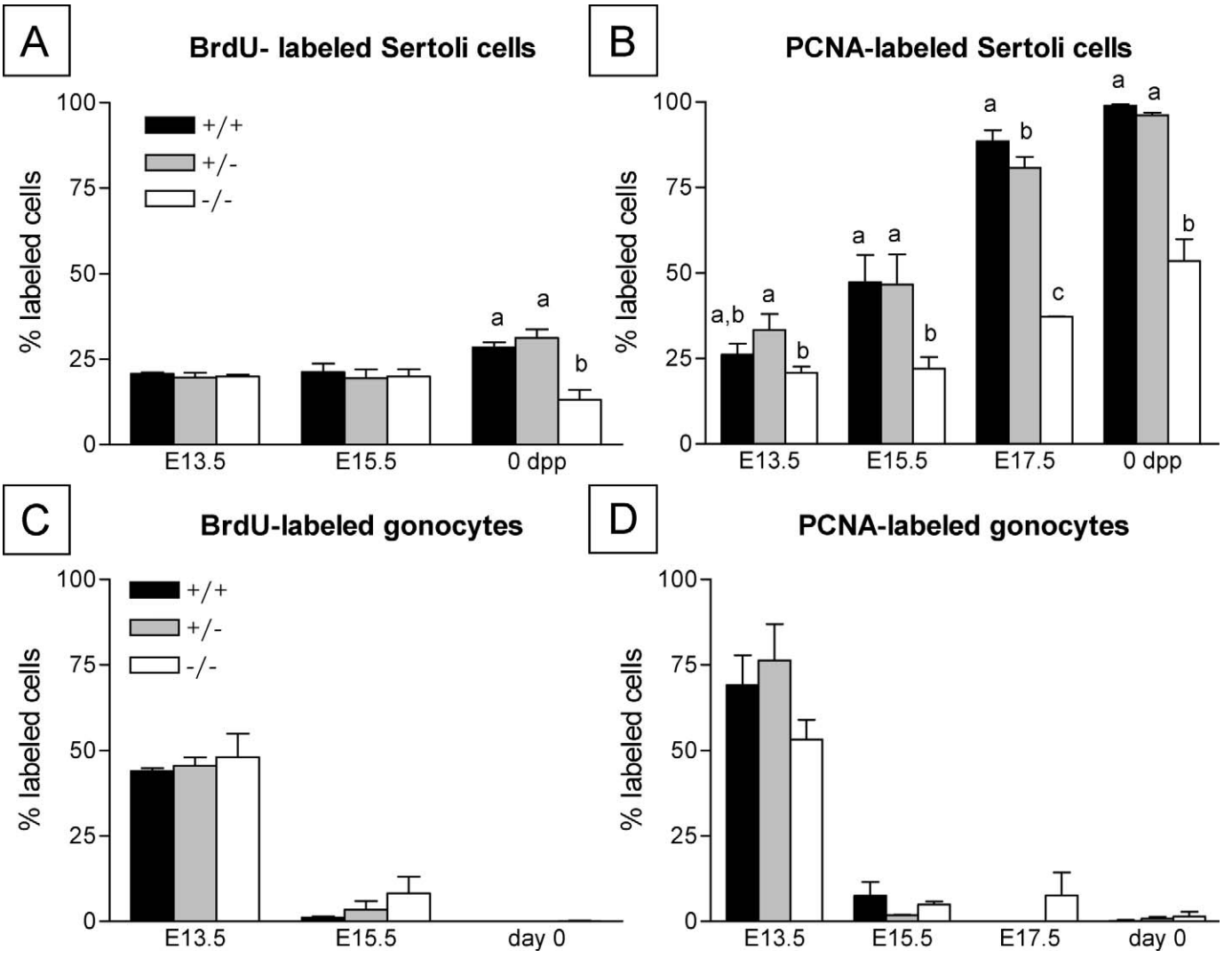

FIG. 3. Effect of *Inhba* dosage on cell proliferation in the fetal mouse testis. Quantitation of Sertoli cell proliferation (**A** and **B**) and gonocyte proliferation (**C** and **D**) using BrdU and PCNA. Labeling indices are presented as percentage of labeled cells. Numbers are supplied in Supplemental Figure S1, including SEM and minimum number of cells counted for BrdU and PCNA. **A**) The percentage of BrdU-labeled Sertoli cells was not significantly different between animals of all three genotypes at E13.5 and E15.5, whereas at 0 dpp there were significantly fewer BrdU-labeled Sertoli cells in $Inhba^{-/-}$ animals compared with both $Inhba^{+/-}$ and $Inhba^{+/+}$ littermates. **B**) The percentage of PCNA-labeled Sertoli cells was significantly lower in $Inhba^{-/-}$ testes compared with $Inhba^{+/-}$ samples at E13.5, whereas $Inhba^{+/+}$ samples were not different. The percentage of PCNA-labeled Sertoli cells was significantly lower in $Inhba^{-/-}$ mice compared with $Inhba^{+/+}$ and $Inhba^{+/-}$ animals at E15.5. At E17.5, $Inhba^{+/-}$ testes exhibited lower proportional PCNA labeling compared with $Inhba^{+/+}$ animals, with an even greater decrease in comparison with $Inhba^{-/-}$ animals. At 0 dpp, the proportion of PCNA-labeled Sertoli cells was significantly lower in $Inhba^{-/-}$ mice compared with both $Inhba^{+/+}$ and $Inhba^{+/-}$ mice, with no difference seen between $Inhba^{+/-}$ and $Inhba^{+/+}$ animals. Letters indicate significant differences ($P < 0.05$) by one-way ANOVA and Newman-Keuls post test, with n = 5 animals for each age and genotype. **C**) The percentage of BrdU-labeled gonocytes decreased dramatically from E13.5 to 0 dpp. Significant differences between animals of different genotypes within each age group were not detected. **D**) The percentage of PCNA-labeled gonocytes was unchanged between animals of different genotypes at each developmental age. However, PCNA-labeled gonocytes were detected at E17.5 in $Inhba^{-/-}$ testes but not in $Inhba^{+/+}$ and $Inhba^{+/-}$ samples. A similar trend outcome was observed for $Inhba^{-/-}$ testes at 0 dpp.

FIG. 4. Activin receptor transcripts and protein in fetal mouse testes. **A**) Activin receptor mRNAs were quantified by real-time PCR using *Actb* as the reference gene and analyzed using the Livak method. The E13.5 $Inhba^{+/+}$ sample value is set to one for all transcript values. Quantitation of transcripts corresponding to activin receptors in the fetal mouse testis by qPCR. All four activin receptor transcripts were the same, regardless of age or genotype at E13.5 and E15.5. At 0 dpp, the *Acvr1* transcript was significantly higher in all three genotypes, whereas *Acvr1b* levels were significantly higher in $Inhba^{+/-}$ samples compared with $Inhba^{+/+}$ and $Inhba^{-/-}$. *Acvr2a* was not different. *Acvr2b* levels at 0 dpp were significantly higher in $Inhba^{-/-}$ samples compared with $Inhba^{+/+}$ and $Inhba^{+/-}$. At each age analyzed, n = 5–10 samples for each genotype. **B**) ACVR2A and ACVR2B immunohistochemistry on testes from E15.5 (top row) and 0 dpp (bottom row) animals. At E15.5 and 0 dpp, ACVR2A is localized to gonocyte cytoplasm and interstitial cells, whereas faint Sertoli cell cytoplasmic stain is detected. At E15.5 and 0 dpp, ACVR2B is localized to gonocyte, interstitial cell, and Sertoli cell cytoplasm. The following testicular cells are represented in the figure: gonocytes, black arrows; Sertoli cell nuclei, black arrowheads; Sertoli cell cytoplasm, black asterisk; and interstitial cells, green arrows. Bar = 50 μm. **C**) P-SMAD2/3 in all cells of the knockout fetal mouse testis. Representative images illustrating P-SMAD2/3 immunostaining in the knockout testis at E13.5, E15.5, and 0 dpp. P-SMAD2/3 was detected in the nuclei of gonocytes (black arrows), Sertoli cells (black arrowheads), peritubular myoid cells (yellow chevrons), and interstitial cells (green arrows). Lower panels represent control sections incubated without primary antibody. All sections are counterstained blue with Harris hematoxylin, with a brown nuclear signal indicating positive reaction. Bar = 50 μm.

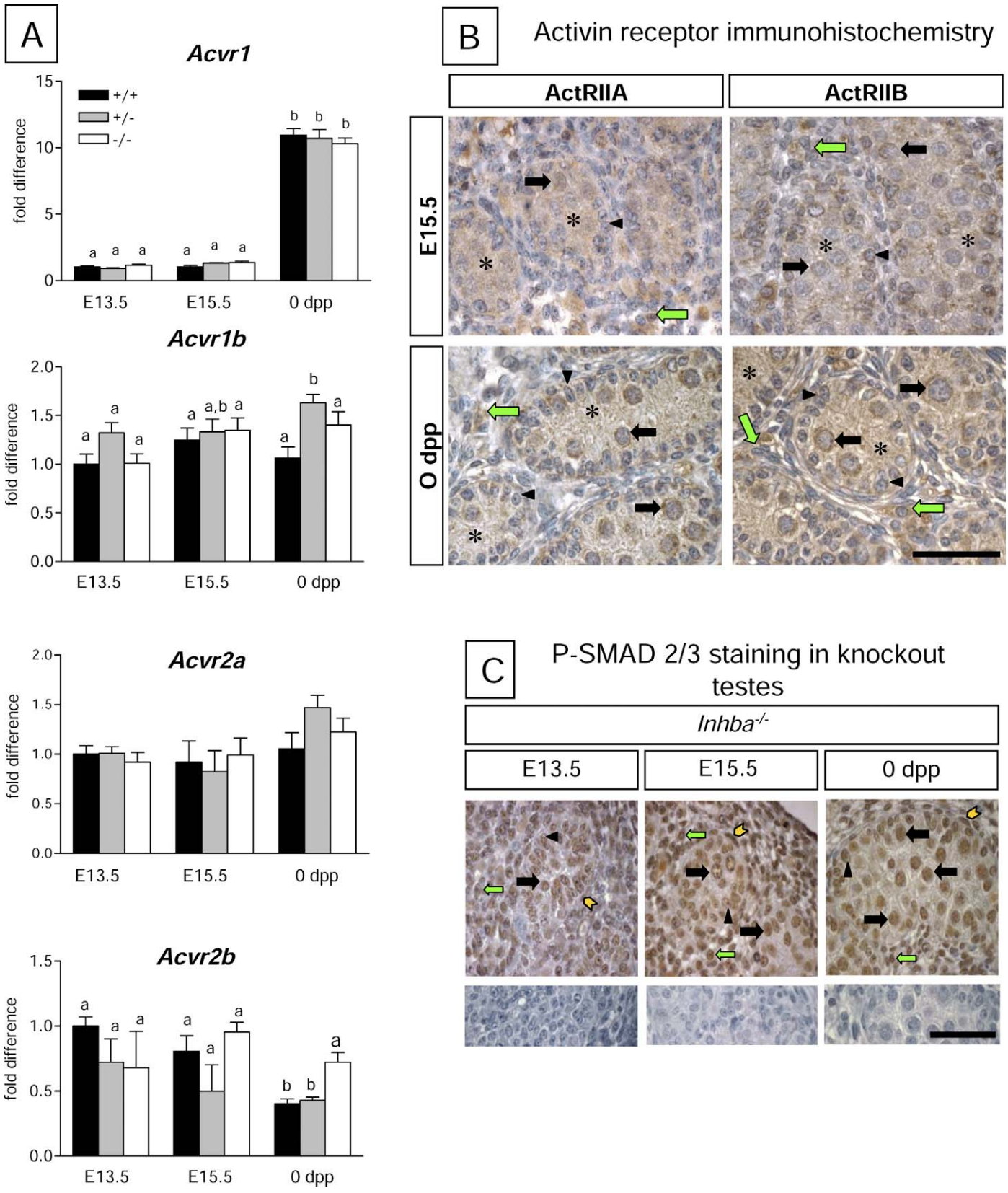

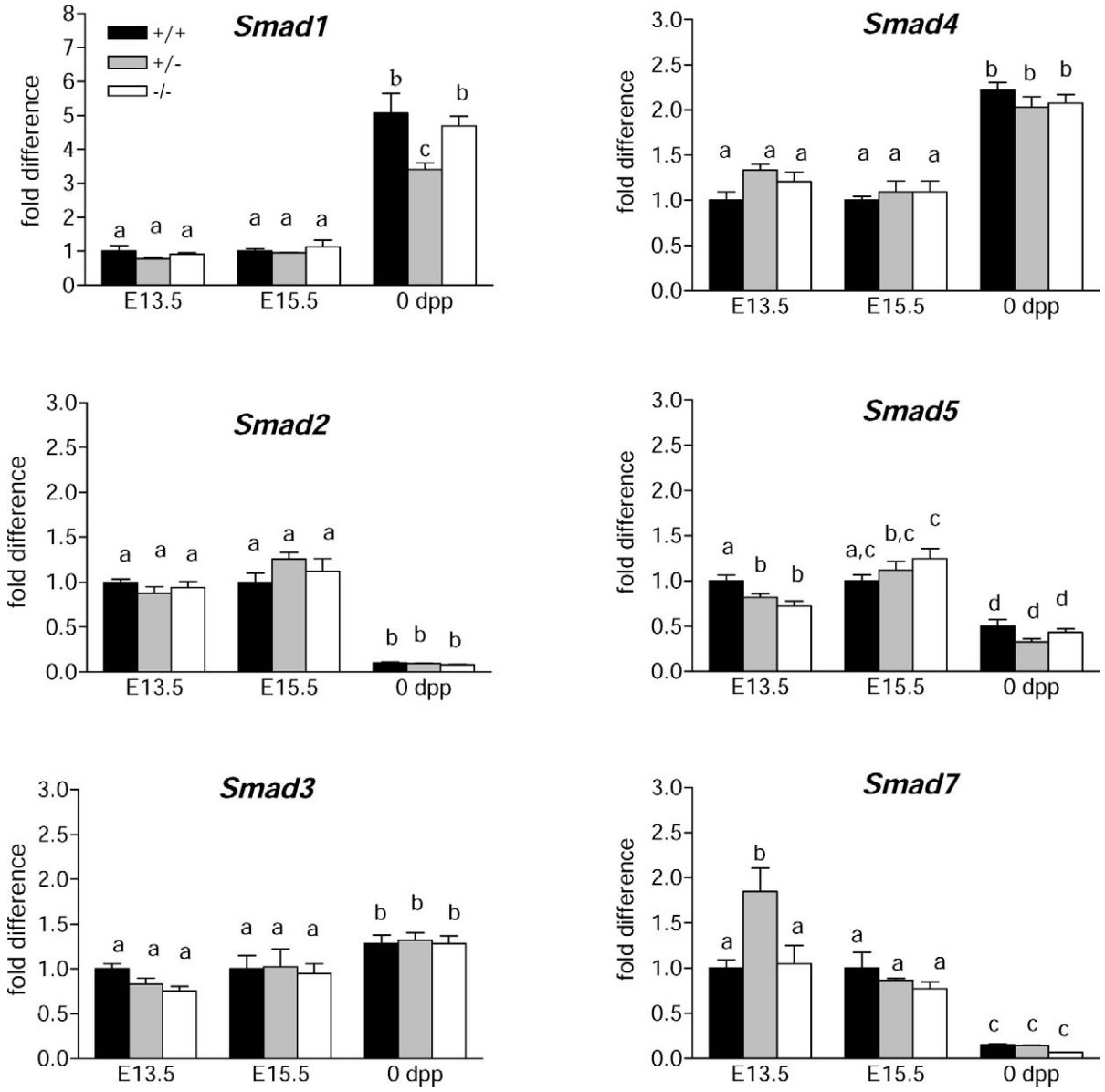

FIG. 5. Smad transcripts in fetal mouse testes. *Smad* mRNAs were quantified by real-time PCR using *Actb* as the reference gene and analyzed using the Livak method. The E13.5 *Inhba*$^{+/+}$ sample value is set to one for all transcript values. Smads 1–4 transcript levels were unchanged regardless of age or genotype at E13.5 and E15.5, whereas *Smad5* and *Smad7* differed in relationship to *Inhba* dosage. At 0 dpp, *Smad1* levels in *Inhba*$^{+/-}$ testes were significantly lower than in *Inhba*$^{+/+}$ and *Inhba*$^{-/-}$. At 0 dpp, *Smad*s *2*, *5*, and *7* were significantly lower in all three genotype groups compared with fetal ages, whereas *Smad3* and *Smad4* transcripts were significantly higher. For each genotype at each age n = 5–10 samples were analyzed. Different letters denote statistically significant differences between all genotypes and age groups by one-way ANOVA ($P < 0.05$) with Newman-Keuls post-test.

Activin Receptors in the Fetal Mouse Testis

Activin receptor qPCR. Based on Affymetrix data [30] and our unpublished data, it was evident that transcripts *Acvr1*, *Acvr1b*, *Acvr2a*, and *Acvr2b* encoding ALK2, ALK4, ActRIIA, and ActRIIB receptor subunits, respectively, were present in the mouse testis. Quantitative PCR was performed to enumerate these transcripts in relationship to age and activin A levels. *Inhba* gene dosage did not affect *Acvr1* mRNA level at any age analyzed (Fig. 4A). However, at 0 dpp, *Acvr1* levels were significantly elevated (10-fold) across all three genotypes compared with fetal ages, indicating that this upregulation occurred between E15.5 and birth. This upregulation corresponds to the period in wild-type testes when Sertoli cell proliferation is at its highest [31]. A less dramatic decrease in the *Acvr2b* transcript level was measured between E15.5 and 0 dpp, and the *Acvr1b* transcript level was significantly higher only in *Inhba*$^{+/-}$ testes at 0 dpp. *Acvr2a* did not vary in relationship to activin dosage or age. Collectively, these data indicate that activin signaling is not altered due to changes in activin receptor subunit synthesis in *Inhba*$^{-/-}$ mouse testes.

Activin receptor and P-SMAD2/3 immunohistochemistry. Both ACVR2A and ACVR2B appear as broadly distributed throughout the fetal testis, being detected in the cytoplasm of Sertoli, gonocyte, and interstitial cells of the E15.5 wild-type testis (Fig. 4B). A similar distribution was evident at 0 dpp, but with relatively more intense gonocyte cytoplasmic staining. The capacity of these antibodies to detect protein bands of the expected mass was verified using Western blot analysis (data not shown). Similar to the wild-type testis (Fig. 1D), P-SMAD 2/3 staining in *Inhba*$^{-/-}$ testes was evident in all cell types (Fig. 4C).

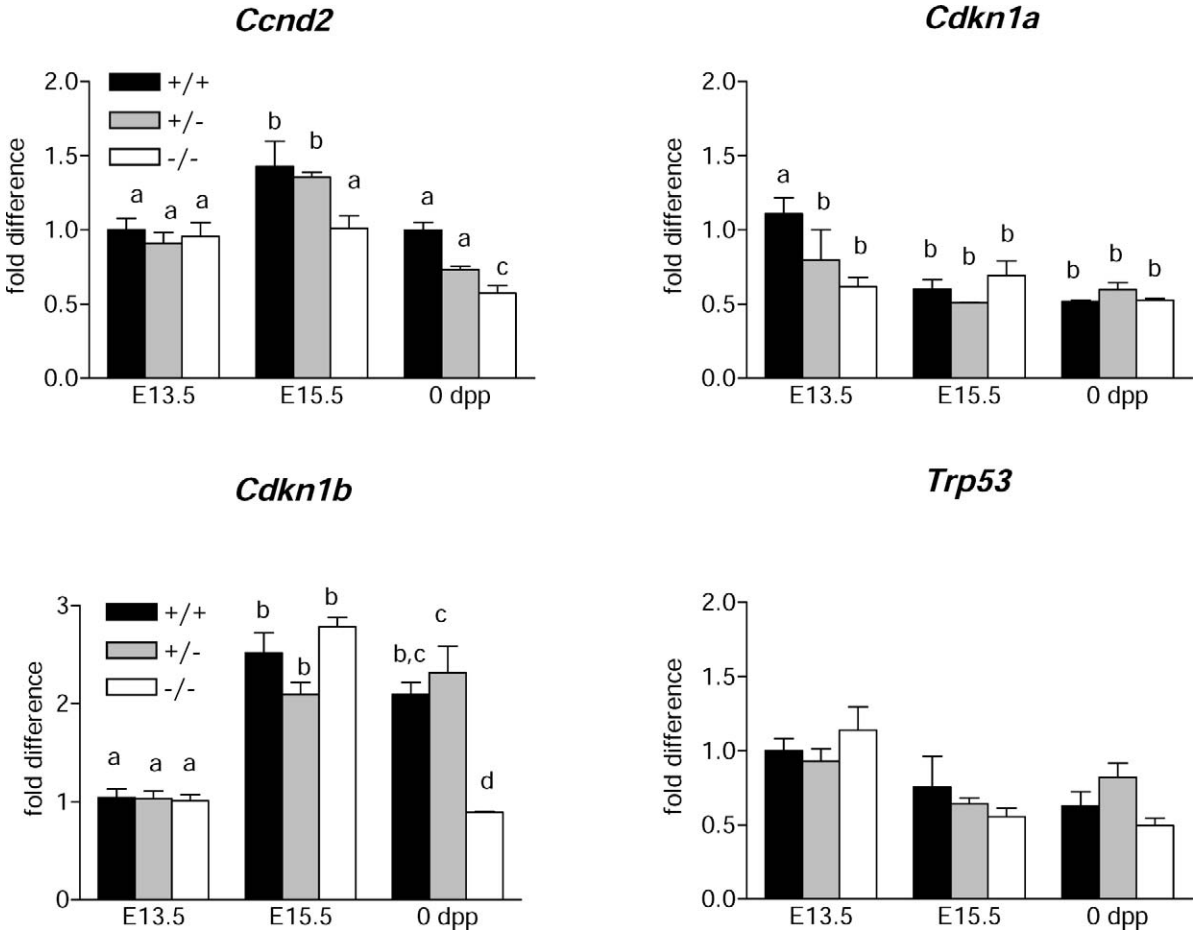

FIG. 6. Cell cycle machinery in the fetal mouse testis. Quantitation of transcripts corresponding to cell cycle machinery in the fetal mouse testis by qPCR. Levels of the *Ccnd2* transcript were not different at E13.5, regardless of *Inhba* dosage. At E15.5 and 0 dpp, $Inhba^{+/+}$ and $Inhba^{+/-}$ transcript levels were significantly higher than in $Inhba^{-/-}$ samples. *Cdkn1a* was not different, regardless of age or *Inhba* gene dosage. The *Cdkn1b* transcript level was not different, regardless of *Inhba* gene dosage at E13.5 and E15.5. However, at 0 dpp, *Cdkn1b* transcript levels were significantly lower in $Inhba^{-/-}$ samples compared with $Inhba^{+/+}$ and $Inhba^{+/-}$ samples. *Trp53* transcript levels were not different, regardless of age or *Inhba* gene dosage. Different letters denote statistically significant differences between all genotypes and age groups by one-way ANOVA ($P < 0.05$) with Newman-Keuls post-test.

Smads in the Fetal Mouse Testis

Quantitative PCR. Quantitative PCR was also used to determine whether Smad transcripts were influenced by age or activin gene dosage using whole mouse testis (Fig. 5). *Smad1* transcript levels were not different at E13.5 and E15.5, regardless of age or *Inhba* dosage. At 0 dpp, *Smad1* was significantly higher in all three genotypes (3- to 5-fold), with $Inhba^{+/-}$ values significantly lower than those in $Inhba^{+/+}$ and $Inhba^{-/-}$ samples. *Smad2* transcript levels were not affected by genotype group at any age analyzed but were significantly lower in all samples at 0 dpp. *Smad3* and *Smad4* were also not affected by genotype at any age analyzed, but in contrast to *Smad2*, they became significantly higher at 0 dpp, with *Smad4* increasing 2-fold relative to fetal ages. Only *Smad5* and *Smad7* transcripts were affected in the fetal testis by genotype. *Smad5* was significantly lower at E13.5 in $Inhba^{+/-}$ and $Inhba^{-/-}$ samples compared with $Inhba^{+/+}$, but was unchanged at E15.5 and 0 dpp relative to *Inhba* gene dosage. The *Smad7* transcript level was significantly higher in $Inhba^{+/-}$ samples only at E13.5 compared with $Inhba^{+/+}$ and $Inhba^{-/-}$. Both *Smad5* and *Smad7* levels were significantly (>50%) lower in all three genotypes at 0 dpp compared with E13.5 and E15.5.

Cell Cycle Machinery

Quantitative PCR. Transcript levels encoding cell cycle regulatory proteins previously implicated in activin signaling were also examined using qPCR in relationship with activin dosage and testis development. *Ccnd2* transcript (encoding cyclin D2) levels did not differ between samples of different genotype at E13.5 but were lower in $Inhba^{-/-}$ testes at E15.5 and 0 dpp compared with $Inhba^{+/+}$ and $Inhba^{+/-}$ samples (Fig. 6). *Cdkn1a* transcripts (encoding $p21^{cip1}$) were significantly lower at E13.5 in $Inhba^{+/-}$ and $Inhba^{-/-}$ samples compared with $Inhba^{+/+}$ ($P < 0.01$), but were not different at E15.5 and 0 dpp. *Cdkn1b* transcripts (encoding p^{27kip1}) were unaffected by activin A dosage at E13.5 and E15.5, but were lower at 0 dpp in $Inhba^{-/-}$ compared with $Inhba^{+/+}$ and $Inhba^{+/-}$ samples. *Cdkn1b* transcripts were increased approximately 2.0- to 2.5-fold between E13.5 and E15.5 across all genotype groups. Transcript levels of *Trp53* (encoding p53) did not differ in relationship to testis age or *Inhba* gene dosage.

Cyclin D2 immunohistochemistry. Cyclin D2 protein (CCND2) was predominantly localized to Sertoli cell nuclei in the E13.5 mouse testis in samples from all three genotypes (Fig. 7). At E15.5, an intense CCND2 signal was present in most nuclei of Sertoli and Leydig cells in all three

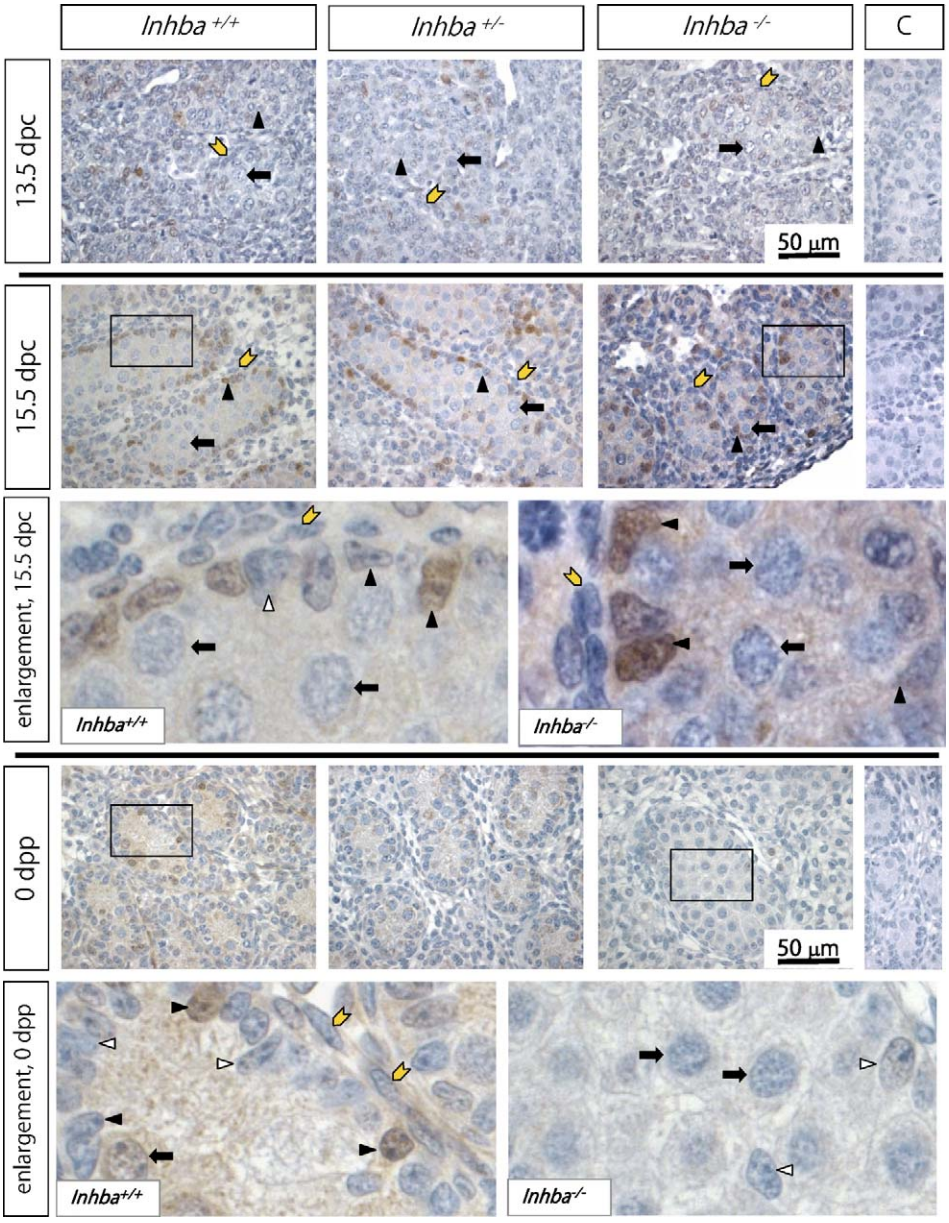

FIG. 7. Cyclin D2 immunohistochemistry. Immunohistochemical detection of cyclin D2 in sections from E13.5 (labeled 13.5 dpc [days postcoitum]), E15.5 (15.5 dpc), and 0 dpp mouse testes. In all samples sections are counterstained blue with Harris hematoxylin, whereas brown staining indicates the presence of CCND2 protein. Panels on the far right represent control (C) sections lacking primary antibody for testes from *Inhba*$^{+/+}$ mice at each age. The following testicular cells are indicated: gonocytes, black arrows; Sertoli cell nuclei, black arrowheads; and peritubular myoid cells, yellow chevrons. Immunohistochemistry was performed twice on two independent samples per age and genotype, with similar results. Bar = 50 µm. Top row: At E13.5, CCND2 protein is detected in Sertoli cell nuclei and Leydig cells in testes of all three genotypes. Gonocytes and peritubular myoid cells are unstained. Second row: At E15.5, CCND2 is not detected in gonocytes, peritubular cells, or Leydig cells, but a majority of Sertoli cell nuclei are stained in samples of all three genotypes. Third row: Enlargement of images from testes of E15.5 *Inhba*$^{+/+}$ mice (left) and *Inhba*$^{-/-}$ mice (right). Several Sertoli cell nuclei are positive for CCND2 protein, with more intense staining in some cells, whereas other nuclei are unstained (white arrowhead). Gonocytes and pertibular cells are unstained. Fourth row: At 0 dpp, cyclin D2 protein is detected in gonocyte cytoplasm and Sertoli cell nuclei, whereas peritubular myoid cells and Leydig cells are unstained. Fifth row: Enlargement of 0 dpp panels in *Inhba*$^{+/+}$ (left) and *Inhba*$^{-/-}$ (right) testes. Gonocyte cytoplasm and Sertoli cell nuclei are positive in *Inhba*$^{+/+}$ testes, whereas staining is absent in *Inhba*$^{-/-}$ testes.

genotypes, with no apparent staining in gonocytes and peritubular myoid cells. Sertoli cell and, rarely, gonocyte nuclei were immunoreactive in 0 dpp *Inhba*$^{+/+}$ samples; however, no protein was detected in any cells in *Inhba*$^{-/-}$ testes (Fig. 7, enlargements).

DISCUSSION

This study identified specific features in fetal and newborn mouse testes that are affected by *Inhba* gene dosage and which collectively implicate activin A in the coordination of somatic and germ cell growth. These are summarized in Figure 8 to show that decreased testis weights at birth in *Inhba*$^{-/-}$ mice correlates directly with decreased Sertoli cell numbers. The contrasting increase in germ cell numbers at birth, although significant, does not appear to influence organ weight due to the relatively low germ cell:Sertoli cell ratio in the fetal and newborn testis.

The analysis presented here demonstrates that the temporal impact of activin actions is different for germ and Sertoli cells. The reduction in Sertoli cell proliferation in *Inhba*$^{-/-}$ mice was not as pronounced at the younger ages analyzed. Sertoli cells proliferate continuously from E12.5 through 10 dpp in the mouse [32], but, remarkably, both BrdU and PCNA labeling revealed that Sertoli cell proliferation in *Inhba*$^{-/-}$ animals had ceased at birth. PCNA labeling proliferation was significantly lower after E15.5, with the same trend demonstrated at E17.5 and 0 dpp. The BrdU labeling, on the other hand, demonstrated that Sertoli cell proliferation was lower in *Inhba*$^{-/-}$ animals at 0 dpp only. This difference may be explained by the parts of the cell cycle that PCNA and BrdU detect. PCNA is a 36-kDa protein subunit of DNA polymerase delta that is essential for both DNA replication and error repair [33, 34]. Maximal expression of PCNA is detected in the G_1 and S phases of the cell cycle, where it interacts with cyclin-dependent kinases involved with cell cycle control [35], decreasing in G_2 and M. The thymidine analogue, BrdU, is incorporated into the elongating DNA chain during the S phase only. Hence, overestimation of cell proliferation is probable with PCNA because it is involved in DNA repair, is present in the early G_0 phase, and has a relatively long half-life of 8–20 h, whereas BrdU incorporation only occurs during S phase [34].

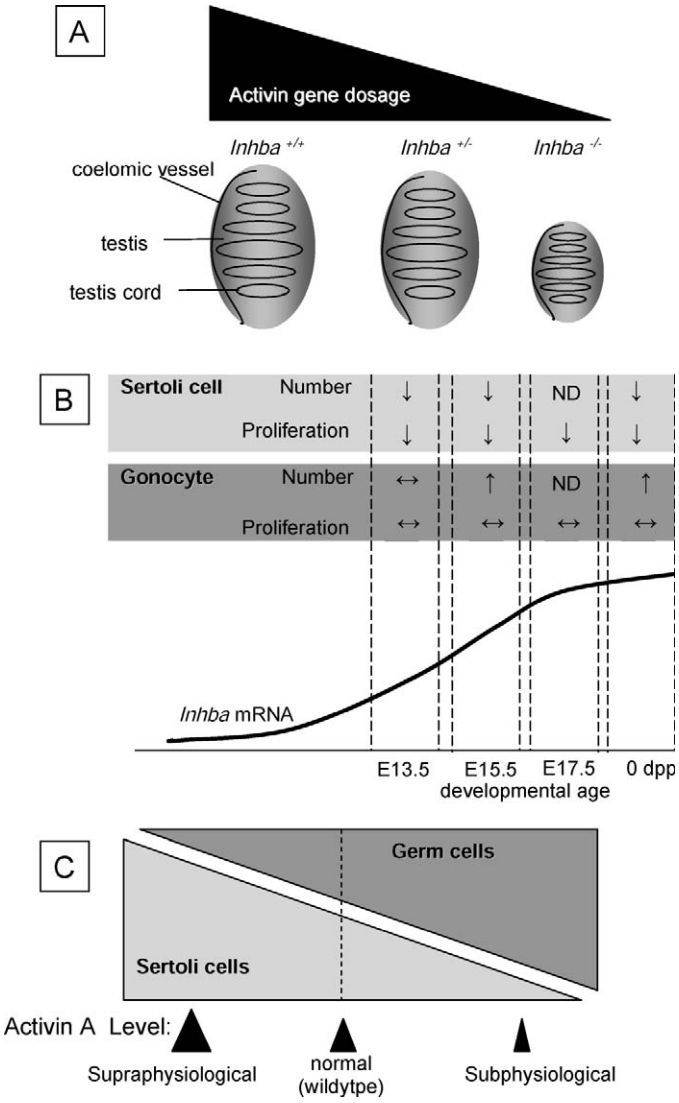

FIG. 8. Phenotype of the activin-deficient mouse testis. Schematic diagrams illustrating changes in testis size and overview of *Inhba* influence on Sertoli and germ cell compartments in the fetal mouse testis (**A**), and more detailed information showing cellular proliferation and cord parameters at each age studied when *Inhba* is absent (**B**). **A**) As *Inhba* gene dosage decreases from two copies in $Inhba^{+/+}$ animals to zero in $Inhba^{-/-}$ testes, so too does testis size. Sertoli cells are significantly reduced in the $Inhba^{-/-}$ testis, whereas gonocyte numbers are increased compared with both $Inhba^{+/+}$ and $Inhba^{+/-}$ testes. **B**) Sertoli cell number and proliferation are significantly reduced at all ages in the testes of $Inhba^{-/-}$ animals. Gonocyte number is unchanged, regardless of activin A dosage at E13.5; however, at E15.5, gonocyte numbers were significantly increased in the null animal and remained elevated until 0 dpp. Proliferation indicated the same trend but did not reach statistical significance (↔). Parameters not measured at certain ages are represented by ND. **C**) Summary diagram presenting the hypothetical interplay between Sertoli and germ cell numbers that is mediated by activin A bioavailability. Levels of activin A in the wild-type testis set the balance between the proportion of germ cells and Sertoli cells in the fetal testis, thereby establishing a ratio of these cells that most efficiently supports fertility and testis function. Supraphysiological levels of activin A lead to increased numbers of Sertoli cells and reduced numbers of germ cells, whereas subphysiological levels lead to reduced Sertoli cell numbers and can initially support enhanced germ cell numbers until such time in development when they become dependent on Sertoli cells for support.

Therefore, the difference in Sertoli cell proliferation between the two labeling methods is attributed to differences in the parts of the cell cycle in which they specifically operate. Because BrdU works in a smaller, more discrete time frame than PCNA, it is expected to display a reduced proliferation index. Similarly, a previous study in rat has demonstrated a difference in the percentage of PCNA-labeled Sertoli cells compared with MKI67, showing that two labeling methods have the potential to produce different proliferation percentages [36].

Gonocyte numbers were significantly higher at E15.5 and 0 dpp in $Inhba^{-/-}$ testes compared with wild-type samples. Labeling with BrdU and PCNA did not reveal numerically significant differences in gonocyte proliferation; however, the presence of a small population of proliferating germ cells during the normal period of quiescence was remarkable and consistent. These differences in cell numbers and proliferation corresponded to altered transcriptional activity of a known activin target gene, with a significant difference between wild-type and knockout sample transcripts measured for *Cdkn1a* only at E13.5. This transcript is predominant in the germ cell compartment at E12.5–E15.5 [9] and encodes the $p21^{cip1}$ inhibitor of cyclin-Cdk complexes, which prevents progression through the G_1 cell cycle checkpoint [37]. The significantly reduced *Cdkn1a* transcript level at E13.5 in $Inhba^{-/-}$ testes reveals an important function for the elevation in activin A synthesis, which occurs immediately after sex determination only in the testis. We conclude that the normal impact of activin at this stage is to contribute to the cessation of gonocyte proliferation that is effected by E14.5, with our observation here of increased germ cell numbers at E15.5 and 0 dpp arising from the sustained proliferation of a subset of germ cells identified here by PCNA and BrdU labeling.

Cyclin D2 is one of three D-type cyclins involved in the progression through the G_1 cell cycle checkpoint. Therefore, the reduction in *Ccnd2* transcript previously shown to predominate in the testis somatic cell compartment at E12.5–E15.5 [9] provides a mechanism for the decrease in Sertoli cell proliferation measured in this study. In addition, the absence of detectable cyclin D2 protein in $Inhba^{-/-}$ testes indicated that all Sertoli cell proliferation had ceased in the absence of the activin A subunit. These findings provide the first in vivo demonstration that activin has a stimulatory impact on the fetal Sertoli cell proliferation, in addition to that previously demonstrated in the postnatal rodent testis [29, 38, 39].

Transcripts corresponding to activin receptor subunits were generally unaffected by *Inhba* gene dosage, with *Acvr1* levels rising dramatically between E15.5 and at 0 dpp in testes of all genotypes. Immunohistochemistry results indicate that these receptor subunits are widespread, whereas ubiquitous P-SMAD2/3 staining in wild-type and knockout testes illustrates the prevalence of multiple TGFB superfamily ligand activities in the fetal mouse testis. The ACVR2A and ACVR2B proteins, which were readily observed in the 0 dpp gonocyte cytoplasm, have the capacity to bind a wide range of ligands, including activins A and B; BMPs 1–5; GDFs 1, 8, 9, and 11; AMH; and nodal [40–43]. Discerning which among these can signal in the absence of activin will provide insights into the coordination of signaling inputs that govern fetal testis growth.

Similar to the activin receptor subunits, Smad transcripts did not appear to be influenced by *Inhba* gene dosage. However, *Smad1* and *Smad4* transcript levels were significantly higher and *Smad2*, *Smad5*, and *Smad7* significantly lower in all genotypes at 0 dpp compared with fetal ages. These differences would be expected to mediate different signaling outcomes in response to signaling by a particular ligand. Whereas Smad4 is recruited in all canonical TGFB

pathway signaling events, Smad1 is predominantly associated with BMP, GDF, and AMH, but not activin signaling [41, 44]. In addition to the differences observed between knockout and wild-type samples, heterozygous animals also demonstrated significant *Inhba* dosage effects revealed using qPCR analysis. Analyses of heterozygote animals from other strains of mice with altered activin bioactivity (*Smad3*, *Inhba*^{BK}) in our laboratory have shown that these also have a measurable phenotype compared with wild-type and homozygous mutant littermates. In addition, published data from our laboratory demonstrate that mouse Sertoli cells exposed to activin A at two different concentrations (5 ng/ml versus 50 ng/ml) display different signaling outcomes [45], further evidence that activin actions are dosage dependent. These data collectively suggest that *Inhba* dosage does not have a general effect on transcript levels of the main signaling components in the activin pathway, but instead causes transcriptional changes at specific developmental time points. Using this and other models to understand how the complex milieu of TGFB superfamily signaling components act in the fetal testis is an important challenge that is of relevance to understanding the etiology of testicular cancer in humans [46], where activin and TGFB superfamily receptor subunits, ligands, and inhibitors have been implicated [47, 48].

This study provides evidence that activin modulates organ growth, demonstrating in particular that a newborn testis without activin A is smaller and contains fewer Sertoli cells and more germ cells compared with the normal animal. This observation extends two recent studies which have delineated an impact of altered TGFB superfamily signaling on fetal testis growth in mouse models. Abrogation of TGFB signaling in gonocytes through conditional deletion of the TGFBR2 subunit in germ cells results in a delay in the onset of quiescence [49], as shown here in the absence of the activin βA subunit. In addition, mice with conditional deletion of *Inhba* in fetal Leydig cells display decreased Sertoli cell proliferation and testis cord dysgenesis [14]. In the present study, we have identified the additional outcome of simultaneous phenotypic changes affecting both somatic (Sertoli cell) and germ cells. The *Inhba*$^{-/-}$ testis phenotype is similar to that of testicular feminized mice (*Tfm*), which have an inactivating mutation in the androgen receptor gene [50, 51], and as a consequence exhibit altered androgen signaling [52]. *Tfm* testes contain significantly more BrdU-positive gonocytes at E15.5, and overall more gonocytes at E17.5 compared with wild-type controls. Sertoli cell number is also decreased in *Tfm* mice just after birth compared with controls [53, 54]. In light of the striking similarities between *Inhba*$^{-/-}$ and *Tfm* mice, it would be intriguing to measure transcripts encoding cell cycle regulatory genes in the latter to ascertain whether this model affects common pathways to influence testis growth and the balance between Sertoli and germ cell numbers in fetal life. Analysis of activin target genes in these and other models exhibiting perturbed fetal testis growth will undoubtedly reveal more about the complex interactions that govern organ growth and the establishment of a balance between germ and somatic cells, which is a feature of the fertile testis.

ACKNOWLEDGMENTS

The authors gratefully acknowledge the importance of discussions with Humphrey Yao, which guided initial data observations, and correspondence with Marty Matzuk. We appreciate the careful reading of this manuscript by Catherine Itman and the excellent technical support by Josephine Howden and Jessica Eberbach of the Monash Medical Centre Animal Facility.

REFERENCES

1. Itman C, Mendis S, Barakat B, Loveland KL. All in the family: TGF-beta family action in testis development. Reproduction 2006; 132:233–246.
2. Loveland KL, Robertson DM. The TGF b superfamily in Sertoli cell biology. In: Griswold M, Skinner M (eds.), Sertoli Cell Biology. Maryland Heights, Missouri: Elsevier Science; 2005:227–247.
3. Jorgez CJ, Lin YN, Matzuk MM. Genetic manipulations to study reproduction. Mol Cell Endocrinol 2005; 234:127–135.
4. Vale W, Rivier C, Hsueh A, Campen C, Meunier H, Bicsak T, Vaughan J, Corrigan A, Bardin W, Sawchenko P. Chemical and biological characterization of the inhibin family of protein hormones. Recent Prog Horm Res 1988; 44:1–34.
5. Sinclair AH, Berta P, Palmer MS, Hawkins JR, Griffiths BL, Smith MJ, Foster JW, Frischauf AM, Lovell-Badge R, Goodfellow PN. A gene from the human sex-determining region encodes a protein with homology to a conserved DNA-binding motif. Nature 1990; 346:240–244.
6. Koopman P, Bullejos M, Bowles J. Regulation of male sexual development by Sry and Sox9. J Exp Zool 2001; 290:463–474.
7. Adams IR, McLaren A. Sexually dimorphic development of mouse primordial germ cells: switching from oogenesis to spermatogenesis. Development 2002; 129:1155–1164.
8. Wilhelm D, Palmer SJ, Koopman PA. Sex determination and gonadal development in mammals. Physiol Rev 2007; 87:1–28.
9. Western PS, Miles DC, van den Bergen JA, Burton M, Sinclair AH. Dynamic regulation of mitotic arrest in fetal male germ cells. Stem Cells 2008; 26:339–347.
10. De Rooij DG. Stem cells in the testis. Int J Exp Pathol 1998; 79:67–80.
11. Kaipia A, Toppari J, Huhtaniemi I, Paranko J. Sex difference in the action of activin-A on cell proliferation of differentiating rat gonad. Endocrinology 1994; 134:2165–2170.
12. Olaso R, Pairault C, Boulogne P, Durand P, Habert R. Transforming Growth Factor Beta1 and Beta2 reduce the number of gonocytes by increasing apoptosis. Endocrinology 1998; 139:733–740.
13. Tomaszewski J, Joseph A, Archambeault D, Yao HH. Essential roles of inhibin beta A in mouse epididymal coiling. Proc Natl Acad Sci U S A 2007; 104:11322–11327.
14. Archambeault DR, Yao HH. Activin A, a product of fetal Leydig cells, is a unique paracrine regulator of Sertoli cell proliferation and fetal testis cord expansion. Proc Natl Acad Sci U S A 2010; 107:10526–10531.
15. Loveland KL, Hogarth C, Mendis S, Efthymiadis A, Ly J, Itman C, Meachem S, Brown CW, Jans DA. Drivers of germ cell maturation. Ann N Y Acad Sci 2005; 1061:173–182.
16. Buzzard JJ, Wreford NG, Morrison JR. Thyroid hormone, retinoic acid and testosterone suppress proliferation and induce markers of differentiation in cultured rat Sertoli cells. Endocrinology 2003; 144:3722–3731.
17. Holsberger DR, Jirawatnotai S, Kiyokawa H, Cooke PS. Thyroid hormone regulates the cell cycle inhibitor p27kip1 in postnatal murine Sertoli cells. Endocrinology 2003; 144:3732–3738.
18. Holsberger DR, Buchold GM, Leal MC, Kiesewetter SE, O'Brien DA, Hess RA, Franca LR, Kiyokawa H, Cooke PS. Cell-cycle inhibitors p27Kip1 and p21Cip1 regulate murine Sertoli cell proliferation. Biol Reprod 2005; 72:1429–1436.
19. Yamato K, Takeyoshi K, Ohguchi M, Kizaki M, Ikeda Y, Nishihara T. Activin A induction of cell-cycle arrest involves modulation of Cyclin D2 and p21$^{cip1/waf1}$ in plasmacytic cells. Mol Endocrinol 1997; 11:1044–1052.
20. Matzuk MM, Kumar TR, Vassalli A, Bickenbach JR, Roop DR, Jaenisch R, Bradley A. Functional analysis of activins during mammalian development. Nature 1995; 374:354–356.
21. McClive PJ, Sinclair AH. Rapid DNA extraction and PCR-sexing of mouse embryos. Mol Reprod Dev 2001; 60:225–226.
22. Mandarim-de-Lacerda CA. Stereological tools in biomedical research. Ann Braz Acad Sci 2003; 75:469–486.
23. Andrews JE, Smith CA, Sinclair AH. Sites of estrogen receptor and aromatase expression in the chicken embryo. Gen Comp Endocrinol 1997; 108:182–190.
24. Buzzard JJ, Loveland KL, O'Bryan MK, O'Connor AE, Bakker M, Hayashi T, Wreford NG, Morrison JR, de Kretser DM. Changes in circulating and testicular levels of inhibin A and B and activin A during postnatal development in the rat. Endocrinology 2004; 145:3532–3541.
25. Wreford NG. Theory and practice of stereological techniques applied to the estimation of cell number and nuclear volume in the testis. Microsc Res Tech 1995; 32:423–436.
26. McLachlan RI, Wreford NG, Meachem SJ, De Kretser DM, Robertson DM. Effects of testosterone on spermatogenic cell populations in the adult rat. Biol Reprod 1994; 51:945–955.

27. Rozen S, Skaletsky H. Primer3 on the WWW for general users and for biologist programmers. In: Krawetz S, Misener S (eds.), Bioinformatics Methods and Protocols. Totowa, NJ: Humana Press; 2000:365–386.
28. Livak KJ, Schmittgen TD. Analysis of relative gene expression data using real-time quantitative PCR and the 2(-Delta Delta C(T)) Method. Methods 2001; 25:402–408.
29. Mithraprabhu S, Mendis S, Meachem SJ, Tubino L, Matzuk MM, Brown CW, Loveland KL. Activin bioactivity affects germ cell differentiation in the postnatal mouse testis in vivo. Biol Reprod 2010; 82:980–990.
30. Small CL, Shima JE, Uzumcu M, Skinner MK, Griswold MD. Profiling gene expression during the differentiation and development of the murine embryonic gonad. Biol Reprod 2005; 72:492–501.
31. Orth JM. Proliferation of Sertoli cells in fetal and postnatal rats: a quantitative autoradiographic study. Anat Rec 1982; 203:485–492.
32. Joyce KL, Porcelli J, Cooke PS. Neonatal goitrogen treatment increases adult testis size and sperm production in the mouse. J Androl 1993; 14: 448–455.
33. Bravo R, Frank R, Blundell PA, MacDonald-Bravo H. Cyclin/PCNA is the auxiliary protein of DNA polymerase-d. Nature 1987; 326:515–517.
34. Zacchetti A, Van Garderen E, Teske E, Nederbragt H, Dierendonck JH, Rutteman GR. Validation of the use of proliferation markers in canine neoplastic and non-neoplastic tissues: comparison of KI-67 and proliferating cell nuclear antigen (PCNA) expression versus in vivo bromodeoxyuridine labelling by immunohistochemistry. APMIS 2003; 111:430–438.
35. Bravo R, MacDonald-Bravo H. Existence of two populations of cyclin proliferating cell nuclear antigen during the cell cycle: association with DNA replication sites. J Cell Biochem 1987; 105:1549–1554.
36. Angelopoulou R, Balla M, Lavranos G, Chalikias M, Kitsos C, Baka S, Kittas C. Sertoli cell proliferation in the fetal and neonatal rat testis: a continuous phenomenon? Acta Histochemica 2008; 110:341–347.
37. Holsberger DR, Cooke PS. Understanding the role of thyroid hormone in Sertoli cell development: a mechanistic hypothesis. Cell Tissue Res 2005; 322:133–140.
38. Boitani C, Stefanini M, Fragale A, Morena AR. Activin stimulates Sertoli cell proliferation in a defined period of rat testis development. Endocrinology 1995; 136:5438–5444.
39. Fragale A, Puglisi R, Morena AR, Stafanini M, Boitani C. Age-dependent activin receptor expression pinpoints activin A as a physiological regulator of rat Sertoli cell proliferation. Mol Hum Reprod 2001; 7:1107–1114.
40. Chang H, Brown CW, Matzuk MM. Genetic analysis of the mammalian transforming growth factor-beta superfamily. Endocr Rev 2002; 23:787–823.
41. Mazerbourg S, Sangkuhl K, Luo CW, Sudo S, Klein C, Hsueh AJ. Identification of receptors and signaling pathways for orphan bone morphogenetic protein/growth differentiation factor ligands based on genomic analyses. J Biol Chem 2005; 280:32122–32132.
42. Mazerbourg S, Klein C, Roh J, Kaivo-Oja N, Mottershead DG, Korchynskyi O, Ritvos O, Hsueh AJ. Growth differentiation factor-9 signaling is mediated by the type I receptor, activin receptor-like kinase 5. Mol Endocrinol 2004; 18:653–665.
43. Sieber C, Ploger F, Schwappacher R, Bechtold R, Hanke M, Kawai S, Muraki Y, Katsuura M, Kimura M, Rechtman MM, Henis YI, Pohl J, et al. Monomeric and dimeric GDF-5 show equal type I receptor binding and oligomerization capability and have the same biological activity. Biol Chem 2006; 387:451–460.
44. Heldin CH, Miyazono K, ten Dijke P. TGF-beta signalling from cell membrane to nucleus through SMAD proteins. Nature 1997; 390:465–471.
45. Itman C, Small C, Griswold M, Nagaraja AK, Matzuk MM, Brown CW, Jans DA, Loveland KL. Developmentally regulated SMAD2 and SMAD3 utilization directs activin signaling outcomes. Dev Dyn 2009; 238:1688–1700.
46. Loveland KL, Dias V, Meachem S, Rajpert-deMeyts E. The transforming growth factor-β superfamily in spermatogenesis and testicular dysgenesis. Int J Androl 2007; 30:377–384.
47. Dias V, Meachem S, Rajpert-De Meyts E, McLachlan R, Manuelpillai U, Loveland KL. Activin receptor subunits in normal and dysfunctional adult human testis. Hum Reprod 2008; 23:412–420.
48. Dias VL, Rajpert-De Meyts E, McLachlan R, Loveland KL. Analysis of activin/TGFB-signaling modulators within the normal and dysfunctional adult human testis reveals evidence of altered signaling capacity in a subset of seminomas. Reproduction 2009; 138:801–811.
49. Moreno SG, Attali M, Allemand I, Messiaen S, Fouchet P, Coffigny H, Romeo PH, Habert R. TGFbeta signaling in male germ cells regulates gonocyte quiescence and fertility in mice. Dev Biol 2010; 342:74–84.
50. Charest NJ, Zhou ZX, Lubahn DB, Olsen KL, Wilson EM, French FS. A frameshift mutation destabilizes androgen receptor messenger RNA in the Tfm mouse. Mol Endocrinol 1991; 5:573–581.
51. Gaspar ML, Bourgarel P, Meo T, Tosi M. Structure of messenger RNA of androgen receptor in mice and molecular characterization in Tfm mutant [in French]. C R Seances Soc Biol Fil 1991; 185:510–519.
52. Merlet J, Racine C, Moreau E, Moreno SG, Habert R. Male fetal germ cells are targets for androgens that physiologically inhibit their proliferation. Proc Natl Acad Sci U S A 2007; 104:3615–3620.
53. Johnston H, Baker PJ, Abel M, Charlton HM, Jackson G, Fleming L, Kumar TR, O'Shaughnessy PJ. Regulation of Sertoli cell number and activity by follicle-stimulating hormone and androgen during postnatal development in the mouse. Endocrinology 2004; 145:318–329.
54. Tan KA, De Gendt K, Atanassova N, Walker M, Sharpe RM, Saunders PT, Denolet E, Verhoeven G. The role of androgens in sertoli cell proliferation and functional maturation: studies in mice with total or Sertoli cell-selective ablation of the androgen receptor. Endocrinology 2005; 146:2674–2683.